

ASSESSING SYSTEM IMPEDANCE BASED ON DATA REGROUPING

Shuangting Xu¹, Xianyong Xiao¹, Yang Wang¹, Jun Wu²

1) Sichuan University, The College of Electrical and Engineering, Chengdu 610065, China
(sy_uarena@163.com, xiaoxianyong@163.com, fjwang@scu.edu.cn, +86 137 0801 0842)

2) Electric Power Research Institute of State Grid Zhejiang Electric Power Company, Hangzhou 310014, China
(13888847301@139.com)

Abstract

In recent years, assessing supply system impedance has become crucial due to the concerns on power quality and the proliferation of distributed generators. In this paper, a novel method is shown for passive measurement of system impedances using the gapless waveform data collected by a portable power quality monitoring device. This method improves the overall measurement accuracy through data regrouping. Compared with the traditional methods that use the consecutive measurement data directly, the proposed method regroups the data to find better candidates with less fluctuation on the system side. Simulation studies and extensive field tests have been conducted to verify the effectiveness of the proposed method. The results indicate that the proposed method can serve as a useful tool for impedance measurement tasks performed by utility companies.

Keywords: system impedance, passive method, Thevenin equivalent, power system.

© 2021 Polish Academy of Sciences. All rights reserved

1. Introduction

The Thevenin equivalent impedance of the supply system is important data for both utility companies and their customers. The data has many uses, such as calculating short-circuit currents, verifying models of power system networks, fault location and power quality improvements [1–8]. Therefore, a number of supply system impedance measurement methods have been developed. These methods can be classified into two types: active methods and passive methods.

The active methods employ the injection of intentional disturbances to the power system. The disturbances can be generated by connecting specific devices [9–11] or switching existing electric components manually [12–14]. Then resulting network voltage and current responses are used for impedance estimation. Measurement accuracy can be improved by adjusting disturbance energy for different system conditions and locations. But these specific devices are often large, heavy, costly and complex to use. On the other hand, switching existing components may have an undesired impact on the system operation.

The passive methods utilize the natural load fluctuation in power systems. Several passive methods have been proposed in the literature. The method proposed in [15] employs real number-based regression algorithms to estimate the system impedance. Yet, the approaches in [16–24] focus on continuous measurement issues along with the solutions. However, if there are background variations on the system side, these methods cannot provide satisfactory results. The methods in [25] utilize the linear regression technique and associated data selection to improve estimation accuracy, but it has been found that no results can be provided by these methods in many field cases due to system variation. References [26–29] attempt to address the system variation by assuming that the fluctuation of the load side and the system side are independent. This assumption, however, only holds for harmonic frequencies, while this paper focuses on the system impedance at the fundamental frequency.

In view of the above, this paper presents a practical and dependable method for impedance estimation. In addition to the circuit theory involved, the techniques of transient removal, data regrouping and selection of good estimates are introduced, which is developed for addressing practical issues encountered in field cases. The remainder of this paper is organized as follows: Section 2 describes the problem of system impedance measurement. Section 3 presents the proposed method. Sections 4 and 5 evaluate the performance and effectiveness of the proposed method using simulation and the field data. Finally, conclusions are drawn in Section 6.

2. The problem of system impedance measurement

The problem of system impedance measurement can be understood with the help of Fig. 1. As shown in Fig. 1a, a portable power quality (PQ) monitoring device is placed at a location of the distribution system. A typical location is the service entrance point of a customer or the feeder side of the substation bus. The PQ monitoring device can collect the voltage and current waveforms at its location. The objective here is to determine or estimate the upstream equivalent circuit impedance seen at the monitor location, using the recorded voltage and current waveforms.

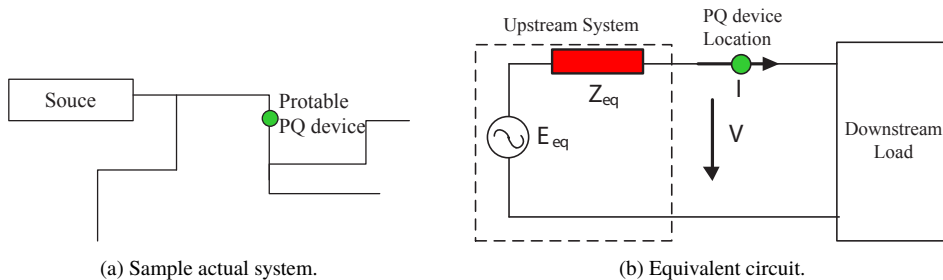


Fig. 1. Defining the problem of system impedance measurement.

The equivalent circuit of the generic system is shown in Fig. 1b. The circuit reveals two variables in the equivalent circuit, E_{eq} is the equivalent source and Z_{eq} is the equivalent source impedance. Z_{eq} is the variable to be estimated.

Since there are two unknowns, E_{eq} and Z_{eq} , in the upstream circuit, two equations are needed to solve for Z_{eq} . To create these two equations, we can assume that (1) the downstream loads have some variations and (2) the upstream side is constant during this period. At instant t_1 , V_1 and I_1

are measured and at instant t_2 , V_2 and I_2 are measured. The following equations can therefore be established:

$$\begin{aligned} E_{eq} &= Z_{eq}I_1 + V_1, \\ E_{eq} &= Z_{eq}I_2 + V_2. \end{aligned} \quad (1)$$

Solving the equations above leads to

$$Z_{eq} = -\frac{V_2 - V_1}{I_2 - I_1} = -\frac{\Delta V}{\Delta I}. \quad (2)$$

In summary, in order to estimate the equivalent network impedance, a variation or disturbance to the voltage and current at the metering point is required. The disturbance can only be caused by the downstream loads or equipment. The system side cannot change, *i.e.* E_{eq} and Z_{eq} must be constants during the measurement period.

Although the theory of system impedance estimation as explained above is straightforward, two problems must be solved. One problem is how to determine the degree and frequency of voltage/current variations that are adequate for impedance estimation. Note that this question can only be answered using actual field measurement data. Different loads have different fluctuation levels. Simulation studies do not show the levels and characteristics of voltage/current variations actually occurring in power systems. Therefore, any research on impedance estimation that is based only on simulated results may not be able to pass the reality test. It is essential to test any proposed methods on field data. The other problem is how to separate the variations caused by the upstream system from those caused by the downstream system. As explained earlier, only downstream disturbances shall be used for impedance estimation.

3. The proposed method

To address the challenges mentioned in the previous section, an improved passive impedance estimation method has been proposed. The proposed method is explained below.

3.1. The basic algorithm

The proposed algorithm of system impedance estimation is built on the work presented in [25]. Assuming that the system remains constant for a group of data (*i.e.* N samples),

$$\begin{cases} E_{eq} = Z_{eq} \times I_1 + V_1 \\ E_{eq} = Z_{eq} \times I_2 + V_2 \\ \vdots \\ E_{eq} = Z_{eq} \times I_N + V_N \end{cases}. \quad (3)$$

A complex number-based linear least squares regression can be performed to obtain the system impedance. The objective function of the regression is given by

$$\min f(Z_{eq}, E_{eq}) = \sum_{i=1}^N |V_i + Z_{eq} \times I_i - E_{eq}|^2. \quad (4)$$

The solution of (4) is

$$\begin{bmatrix} Z_{eq} \\ E_{eq} \end{bmatrix} = (X^T X)^{-1} X^T Y, \quad (5)$$

$$\text{where } X = \begin{bmatrix} -I_1 & 1 \\ -I_2 & 1 \\ \vdots & \vdots \\ -I_N & 1 \end{bmatrix} \text{ and } Y = \begin{bmatrix} V_1 \\ V_2 \\ \vdots \\ V_N \end{bmatrix}.$$

This paper selects the linear regression as the basic algorithm due to following considerations. First, the linear regression technique does not require the system side to be perfectly constant. The least squares algorithm can reduce the impact of system variations. Second, the linear regression technique is a simple but mature statistical algorithm. Several indices have been developed to check the reliability of the estimates. However, using pure linear regression technique may not yield satisfactory results. Therefore, several improvements are further proposed in the remainder of this section to enhance the accuracy and the reliability of the impedance estimation in real implementation.

3.2. Remove undesirable transients

All passive methods assume the system operates under the steady-state conditions. Otherwise, (1)–(5) are not valid. This means that the transient data must be removed from the impedance estimation. To the authors' best knowledge, this practical issue has not been discussed nor addressed in any literature. The typical duration of the transient events is less than 3 fundamental cycles, as per IEEE 1159-2019 [30]. Due to the existence of system damping, the transient is generally attenuated; that is, the values of different cycles vary with the time. If a transient event occurs, the corresponding current phasor in the adjacent cycle will change. Therefore, this paper proposes removing the transient data by comparing the current phasors. Discrete Fourier transform (DFT) is applied for three consecutive cycles and the variation ratios of consecutive two phasors are calculated as follows:

$$\left| \frac{I_{i+1} - I_i}{I_i} \right| < 1\% \ \wedge \ \left| \frac{I_{i+2} - I_{i+1}}{I_{i+1}} \right| < 1\%, \quad (6)$$

where I_i is the first cycle's current phasor, I_{i+1} is the second cycle's current phasor and I_{i+2} is the third cycle's current phasor. If the variation ratios in (6) are both less than 1%, I_{i+1} is considered as a steady-state value. If not, I_{i+1} is eliminated and next three consecutive cycles I_{i+1} , I_{i+2} , I_{i+3} are considered.

It should be noted the DFT is biased by the spectral leakage for non-coherent sampling. To solve the issue, this paper describes the use of the coherent resampling method from [31]. The algorithm uses an extended Kalman filter for instantaneous frequency tracking and fractional B-spline resampling for signal approximation. Coherent resampling analysis is performed before the DFT to eliminate the effect of spectral leakage.

3.3. Data regrouping

In (3), it is assumed that both the system impedance (Z_{eq}) and the Thevenin equivalent voltage (E_{eq}) are constant. This is important because when one conducts linear regression calculations between two variables, no other variables should change. However, this assumption may not hold in practice as E_{eq} is likely to have small variations even within a few cycles mainly due to the upstream load fluctuation. For example, if the measurement is taken at a substation feeder, the load variations of all other feeders will result in the fluctuation of E_{eq} . It is thus practically difficult

to find 10 or more consecutive cycles with negligible system variations. This is the main reason why simply using the linear regression technique cannot yield reliable results in many field cases.

The system voltage E_{eq} generally fluctuates within a small range. Finding 10 or more consecutive cycles with equal E_{eq} could be challenging unless the load variation is sufficiently large. Since the supply system impedance is unlikely to change significantly within a short time such as one minute, it is not necessary to constrain the linear regression analysis for consecutive measurements. A data regrouping technique is proposed to find several data samples within a short time that are most likely to have equal E_{eq} , as shown in Fig. 2. The steps are as follows.

1. Select one data sample k (k starts from 1) in the output unit as the target sample. The default output unit can be selected as one minute.
2. For the rest of the samples in the output unit, filter out the phasors which do not satisfy (7). Equation (7) is a necessary condition that there are load changes between the sample k and the sample j . If one sample fails to satisfy (7), it means the load variation is small when compared the fluctuation of E_{eq} . The remaining data samples are called companion samples.

$$\begin{cases} R = \text{real}(Z_{eq}(k, j)) > 0 \\ X = \text{imag}(Z_{eq}(k, j)) > 0 \end{cases}, \quad (7)$$

where

$$Z_{eq}(k, j) = -\frac{V(k) - V(j)}{I(k) - I(j)}. \quad (8)$$

3. The companion samples with similar $Z_{eq}(k, j)$ are most likely to have equal E_{eq} . Therefore, all companion samples are sorted based on the magnitude of $Z_{eq}(k, j)$ and the linear regression analysis is performed for every 9 consecutive companion samples with the target sample k .
4. Once the data regrouping is done for the target data k , select $k + 1$ data as the target data and go to Step 2.

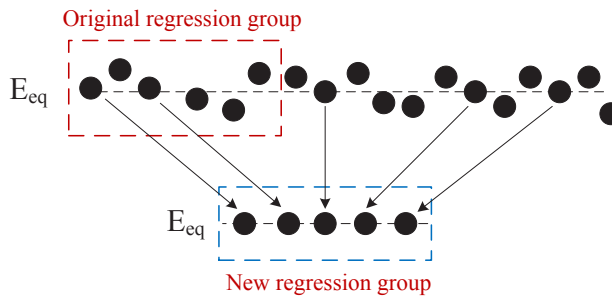


Fig. 2. Data regrouping for the regression analysis.

3.4. Selection of good estimates

If one regression group has an approximately equal E_{eq} , there should be a strong linear correlation between the measured voltage and current, and the corresponding impedance samples can be selected as useable samples; otherwise, these samples should be discarded. The coefficient of determination, namely R^2 , is a statistical index developed to measure how strong the linear

relationship is between the two studied variables, which is defined as

$$R^2 = 1 - \frac{\sum_{i=1}^N |\hat{E}_{eq} - I_i \hat{Z}_{eq} - V_i|^2}{NCov(V)}, \quad (9)$$

where the symbols with hats mean the estimated value, \hat{E}_{eq} , \hat{Z}_{eq} represent the estimated results of the system side voltage and impedance, respectively.

The stronger the linear relationship is, the closer the value of R^2 is to one, so that the more accurate of the estimated impedance is. In practice, estimation results satisfying $R^2 > 0.9$ are commonly regarded as useable results. However, it should be realized that the reliability of R^2 relies on the variance of input data. In the linear regression problem $y = ax + b$, regression coefficient a is determined by studying the inter-dependency between the variation of explanatory variables x and their response to the response variable y . If the fluctuation of x is very small, its response to y becomes ambiguous. It becomes difficult for the linear regression algorithm to determine the correlation between x and y and R^2 may give the wrong result. A simple diagram, as shown in Fig. 3, is plotted below for a better illustration.

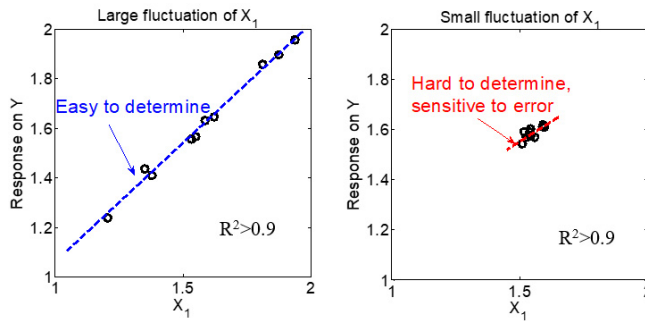


Fig. 3. The impact of the fluctuation of X_1 on the correlation determination.

The analysis above indicates that the useable estimates with larger variance of the current, denoted as $\text{var}(I)$, are considered to be more reliable. Through the data regrouping technique proposed in previous subsection, it is possible to obtain thousands of useable estimates. In this paper, 10% of good estimates with the largest $\text{var}(I)$ are selected as the candidate results, as shown in Fig. 4. These candidate results are finally checked by a statistical test. If the maximum offset of

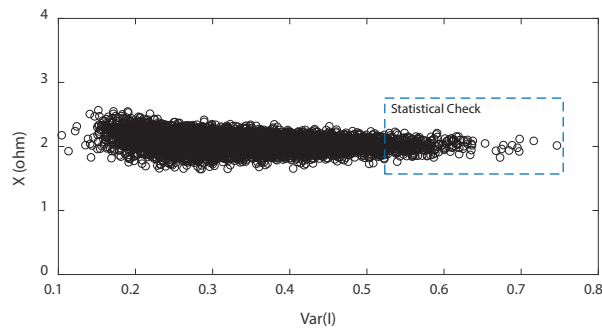


Fig. 4. Estimated impedance convergence characteristic.

the candidate results is within 10% of their mean value, it can be concluded that they are reliable and their mean value can be trusted. Otherwise, the program will tell the user that there are no reliable estimated line parameters that can be given for this output unit.

3.5. Flow chart of the final algorithm

Combining the circuit theory above and practical considerations, the proposed method is implemented in the following steps:

Step 1. Capture three-phase voltage and current waveforms continuously with proper sampling rate, for example, 64 samples per cycle.

Step 2. Each minute is used as a basic unit for impedance result output. If the number of outputs after data selection in Step 3 is small for every minute, a larger basic unit can be used. For each one-minute window, do the following:

Step 2.1. Perform coherent resampling with the method from [31].

Step 2.2. Convert each cycle of the waveforms to the frequency domain using the DFT.

Step 2.3. Remove the undesirable transients data as per (6).

Step 2.4. Convert the resulting three-phase voltage and current phasors to positive-, negative and zero-sequence quantities.

Step 2.5. Select one data sample k (k starts from 1) as the target sample.

Step 2.6. For the rest of the samples in this output unit, filter out the phasors that do not satisfy (7). The remaining samples are called companion samples.

Step 2.7. Sort all companion samples based on their magnitude of $Z_{eq}((k, j))$ and perform the linear regression analysis for every 9 consecutive companion samples with the target sample k . If the impedance estimates do not satisfy $R^2 > 0.9$, reject the result.

Step 2.8. If the calculations are not done for the 1 minute data, select the sample $k + 1$ as the target point and go to Step 2.6.

Step 3. Select 10% useable estimates with the largest variance of the current in this minute as the candidate results.

Step 4. Define the acceptable offset range (e.g. 10%). If the maximum offset of the candidate results is beyond the defined range, go to Step 1.

Step 5. Calculate the average value of the candidate results as the final result of this minute.

Step 6. Go to Step 1.

4. Simulation verification

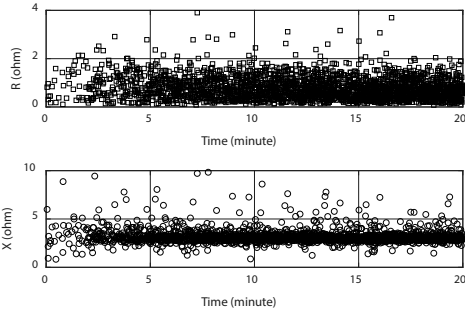
4.1. Performance comparison

It is obvious that all existing methods can provide accurate results when the system is ideally stable. Thus, the focus of simulation verification is to study the impact of the system variations on different methods. In the simulation study, the equivalent circuit model represented in Fig. 1b is simulated to evaluate the effectiveness of the proposed method. The parameter setting is shown in Table 1.

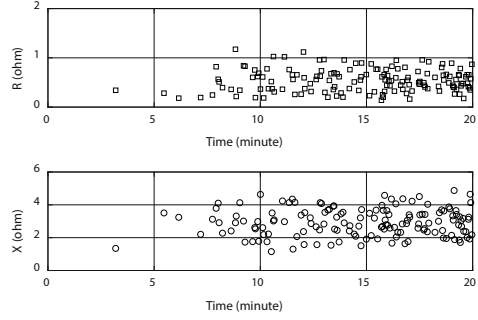
The simulation lasted for 20 minutes and the total of 6000 phasors were generated. The system impedance was estimated by proposed method and typical passive methods (method based on $\alpha-\beta-0$ transformation [22], method based on nonlinear least squares [23], method based on VI determinant [24], method based on data selection [25]). The results are shown in Fig. 5, and

Table 1. Parameter setting in the simulation study.

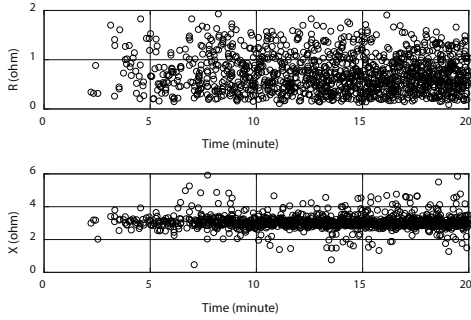
Variable	Magnitude		Phase Angle	
	Mean value	Maximum Variation	Mean value	Maximum Variation
E_{eq}	14.4 kV	0.1%	0 degree	0.01 degree
Z_{eq}	3 ohms	0%	80 degree	0 degree
Z_L	50 ohms	0.05%~10% with a 0.05% step	10 degree	0.05~1 degree with a 0.05-degree step



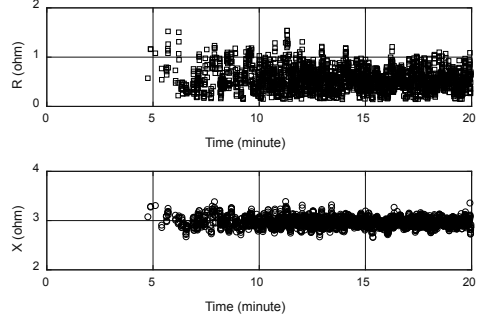
(a) Method based on α - β -0 transformation (Z_α).



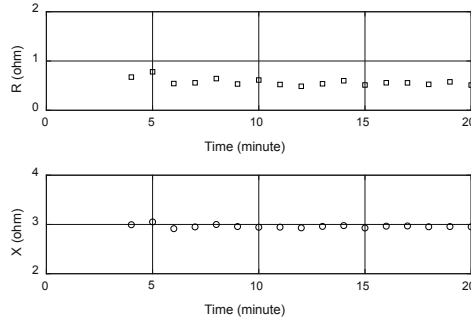
(b) Method based on nonlinear least squares.



(c) Method based on VI determinant.



(d) Method based on data selection.



(e) The proposed method.

Fig. 5. System impedances estimated results.

the mean and standard deviation of R and X are shown in Table 2. It can be seen that: 1) the method based on $\alpha-\beta-0$ transformation has poor estimation accuracy. 2) the method based on nonlinear least squares, and the method based on VI determinant have similar performances. The results are close to the reference value ($0.52 + 2.95j$), but have large fluctuation; 3) The method based on data selection has better accuracy, but certain variations still can be observed, especially in the estimated resistance part. Such a result indicates that system variations have a significant impact on impedance measurement; 4) The results obtained with the proposed method are more accurate than those yielded by the existing methods when the system is not ideally stable. However, for the first three minutes, no reliable results can be provided even by using data regrouping techniques. This is because the load fluctuation is too small in the first few minutes.

Table 2. System impedance estimated results of the proposed method.

Methods	Mean Value		Standard Deviation Value	
	R	X	R	X
Reference value	0.52	2.95	–	–
$\alpha-\beta-0$ transformation	1.83	6.03	4.50	11.09
nonlinear least square	0.60	2.96	0.23	0.89
VI determinant	0.75	3.19	0.93	3.02
data selection	0.62	3.02	0.88	0.68
The proposed method	0.57	2.96	0.07	0.03

4.2. Verification of removing transients

To further illustrate the effectiveness of the proposed method for removing undesirable transients in different scenarios, a simulation case is built in PSCAD/EMTDC as shown in Fig. 6. For this simulation case, two small loads are supplied by an 11 kV feeder and an 11kV-Yg/575 V-Yg transformer. A capacitor bank is connected through breakers. The detailed parameters of components in simulation and the reference value of system impedance at the transformer's secondary side are listed in Table 3. The reference value is obtained by adding the internal impedance of the source feeder and the equivalent impedance of the transformer.

Table 3. Parameters of components in simulation.

No	Name	Parameter
1	Capacitor bank	575 V 200 kVar
2	11 kV source feeder	$0.2 + 2j \Omega$
3	Transformer	1 MVA
4	Load A	500 kW + 300 kVar
5	Load B	50 kW + 30 kVar
6	Reference value of system impedance	$0.0667 + 0.1708j \Omega$

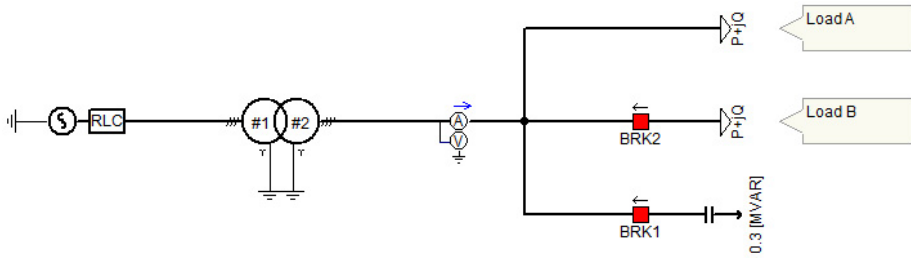


Fig. 6. Diagram of the simulation system.

(1) Capacitor switching

The capacitor bank and Load B are disconnected first. After 0.5 s, the capacitor bank is connected. Three-phase voltage and current waveforms are presented in Fig. 7.

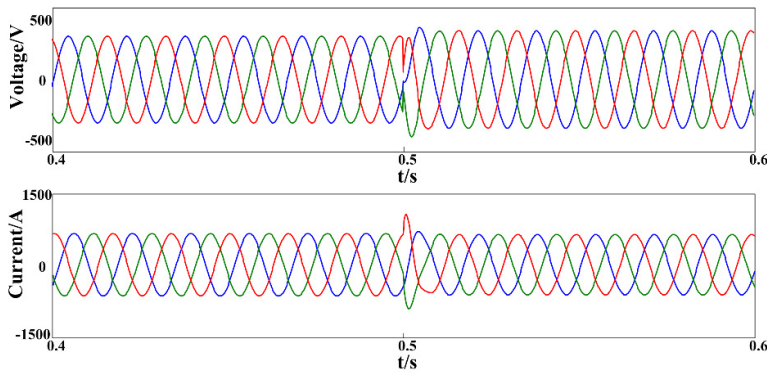


Fig. 7. Three-phase voltage and current waveforms.

The period for which the transient event occurs is defined as i , and the variation ratio is shown in Table 4. The result shows that the cycle $i - 1$, i and $i + 1$ should be filtered out as per (6), that is, the transient data can be excluded. By using the proposed method, the estimated system impedance is $0.0667 + 0.1708j \Omega$, which is consistent with the reference value. If the transient is not removed, the result of the proposed method is $0.2736 + 0.1474j \Omega$.

Table 4. Current phasor in transient event.

Time	Current Phasor	Variation Ratio	
		Previous cycle	Latter cycle
$i - 1$	$-0.4177 - 0.4997j$	0%	39.46%
i	$-0.1878 - 0.6147j$	39.46%	6.82%
$i + 1$	$-0.1441 - 0.6117j$	6.82%	0%

(2) Load variation

Likewise, the capacitor bank and Load B are disconnected first. After 0.5 s, Load B is connected. Three-phase voltage and current waveforms are presented in Fig. 8. Once we define

the period that load B is connected as i , the variation ratio is shown in Table 5. The result shows the cycle $i - 1$, i should be filtered out as per (6). By using the proposed method, the estimated system impedance is $0.0667 + 0.1708j \Omega$, which is consistent with the reference value. If the transient is not removed, the result of the proposed method is $0.0821 + 0.1562j \Omega$. It shows that estimation accuracy can be greatly improved by removing transient data.

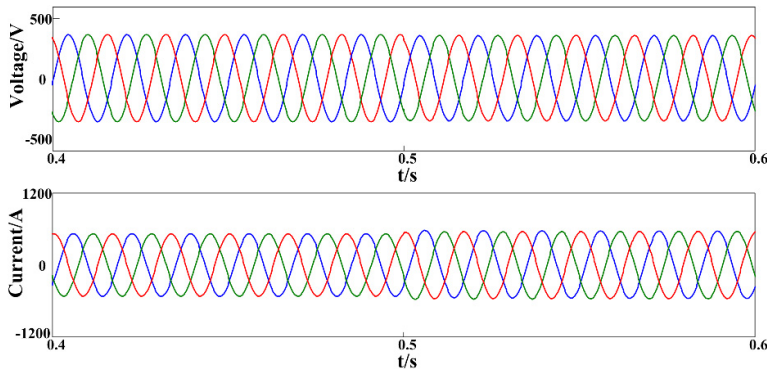


Fig. 8. Three-phase voltage and current waveforms.

Table 5. Current phasor during load variation.

Time	Current Phasor	Variation Ratio	
		Previous cycle	Latter cycle
$i - 1$	$-0.4177 - 0.4997j$	0%	7.74%
i	$-0.4531 - 0.5357j$	7.74%	0.43%
$i + 1$	$-0.4550 - 0.5334j$	0.43%	0.11%
$i + 2$	$-0.4558 - 0.5334j$	0.11%	0%

5. Field data verification

The field measurements are presented in two categories, substation measurements and load side measurements. The estimation results are compared with those calculated using the Power System Simulator for Engineering (PSS/E) short-circuit program. Additionally, results obtained from different feeders are also compared.

5.1. Substation measurements

The substation is a 14.4 kV substation mainly serving commercial loads. An NI-6020E National Instruments 12-bit data-acquisition system with a 15.36 kHz sampling rate controlled by a laptop computer was used for the recording. By using this data-acquisition system, we obtained 256 samples per cycle for three-phase voltages and the waveform of the current at the point of the metering in the load-serving substations. The coherent resampling method in [31] was then applied to address the spectral leakage issue. The three-phase waveforms of each measurement point were transformed to the frequency domain for every cycle, and then, by using the sequence

transformation, the positive- and negative-sequence voltages/currents were calculated. The single-line diagram of the substation and the variation of the RMS values measurement points are shown in Fig. 9.

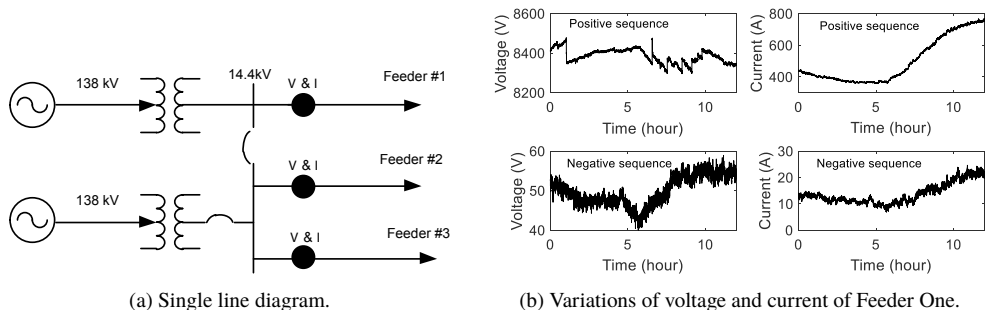


Fig. 9. The system situation of Feeder One.

The system impedance was first estimated by typical passive methods. The results are shown in Fig. 10. As seen from the figures, the method based on $\alpha - \beta - 0$ transformation, the method based on nonlinear least squares, and the method based on VI determinant have similar performances. The results are close to the reference value ($0.12 + 0.85j$), but have large variations. These variations are caused by the change on the system side. The method based on data selection does not provide any results, because no estimates can satisfy the data selection requirement.

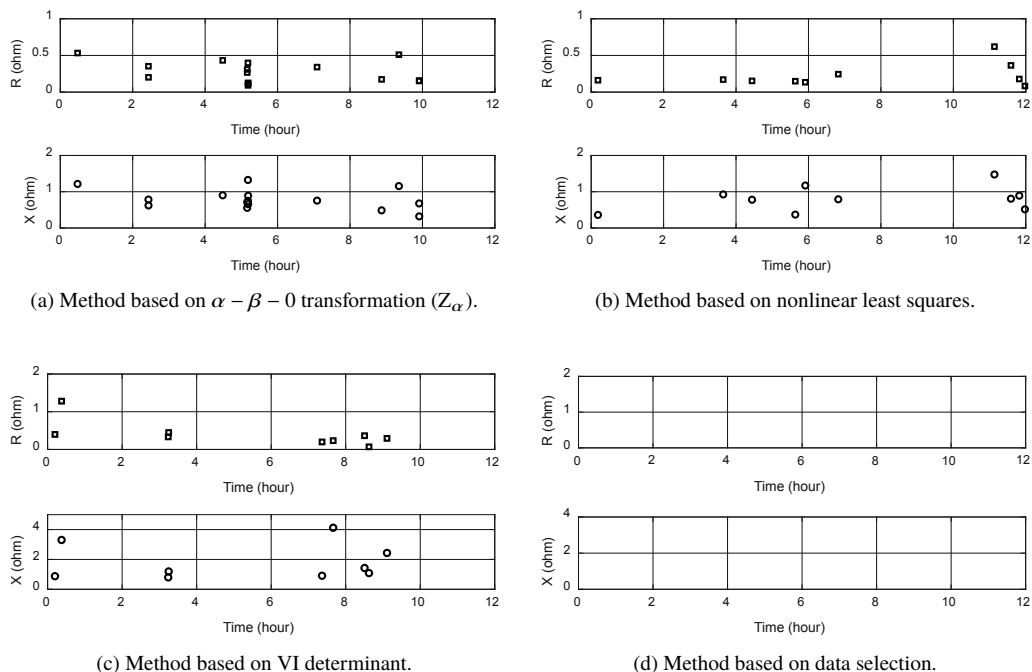


Fig. 10. System impedance estimated results of Feeder One.

The system impedances were then estimated by the proposed method with a group of 10 samples and screened according to the criteria developed earlier. The output for every 10 minutes was plotted in Fig. 11, which shows a stream of estimated impedance data. Compared with Fig. 10d, it can be found that the positive sequence quantities are now able to provide several reliable results owing to the data regrouping technique. On the other hand, estimation based on negative sequence quantities leads to more estimates than that of the positive sequence.

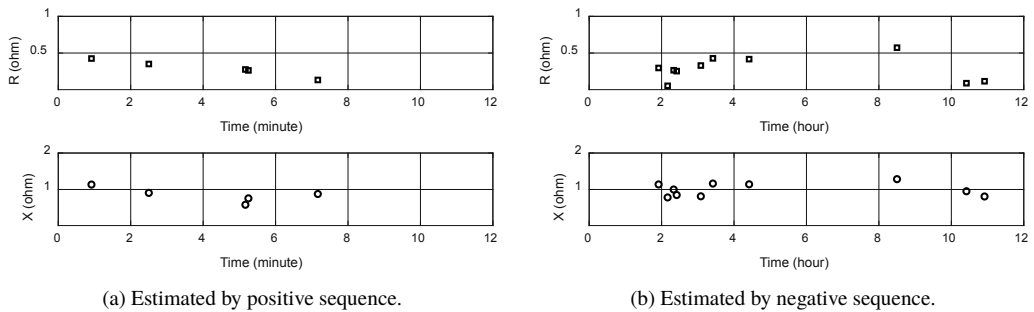


Fig. 11. The System impedance estimated results of Feeder One based on the proposed method.

The proposed algorithm was applied to all the feeders in the substation. The results are shown in Table 6, the average values of the calculated impedances are compared with those derived from the PSS/E model. The agreement is quite acceptable considering that the proposed method uses for impedance estimation only naturally occurring, small disturbances.

Table 6. System impedance data of the Substation.

Feeder	Estimated by Positive Sequence	Estimated by Negative Sequence	PSS/E
# 1	$0.32 + 0.88j$	$0.28 + 0.95j$	$0.12 + 0.85j$
# 2	$0.20 + 0.80j$	$0.16 + 0.84j$	
# 3	NA	$0.25 + 0.93j$	

5.2. Load side measurements

In this paper there are also collected field data from a large load. The measurement was carried out at an oil sand site for around 45 minutes. There are certain load variations during the measurement period mainly caused by the pumpjack operation. The waveforms of three phase voltage and the currents were captured by a Candura Instruments PQpro power quality analyser in the continuous measurement mode. The sampling rate is 256 samples per cycle. The variation of the RMS values of the positive- and negative-sequence voltage/current at the oil sand site is shown in Fig. 12.

System impedance was first estimated by typical passive methods. The results are shown in Figs. 13a–13d. It can be seen that the method based on $\alpha - \beta - 0$ transformation, the method based on nonlinear least squares, and the method based on VI determinant provide lots of impedance estimates in this case due to the large load fluctuation. However, these estimates have large variations which are likely to be caused by the system changes. The method based on

S. Xu et al.: ASSESSING SYSTEM IMPEDANCE BASED ON DATA REGROUPING

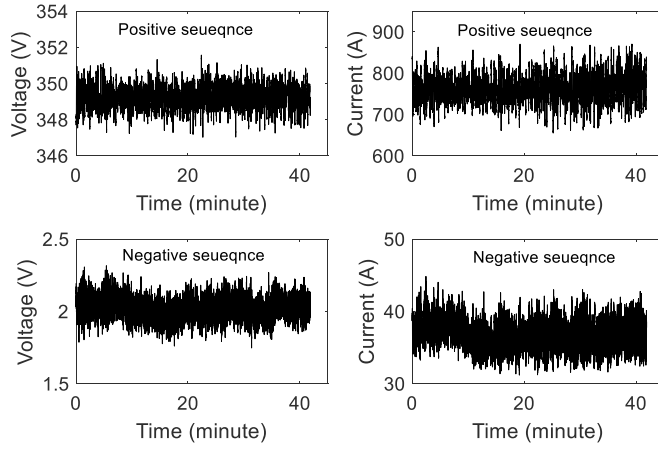


Fig. 12. Variation of voltage and current at the oil sand site.

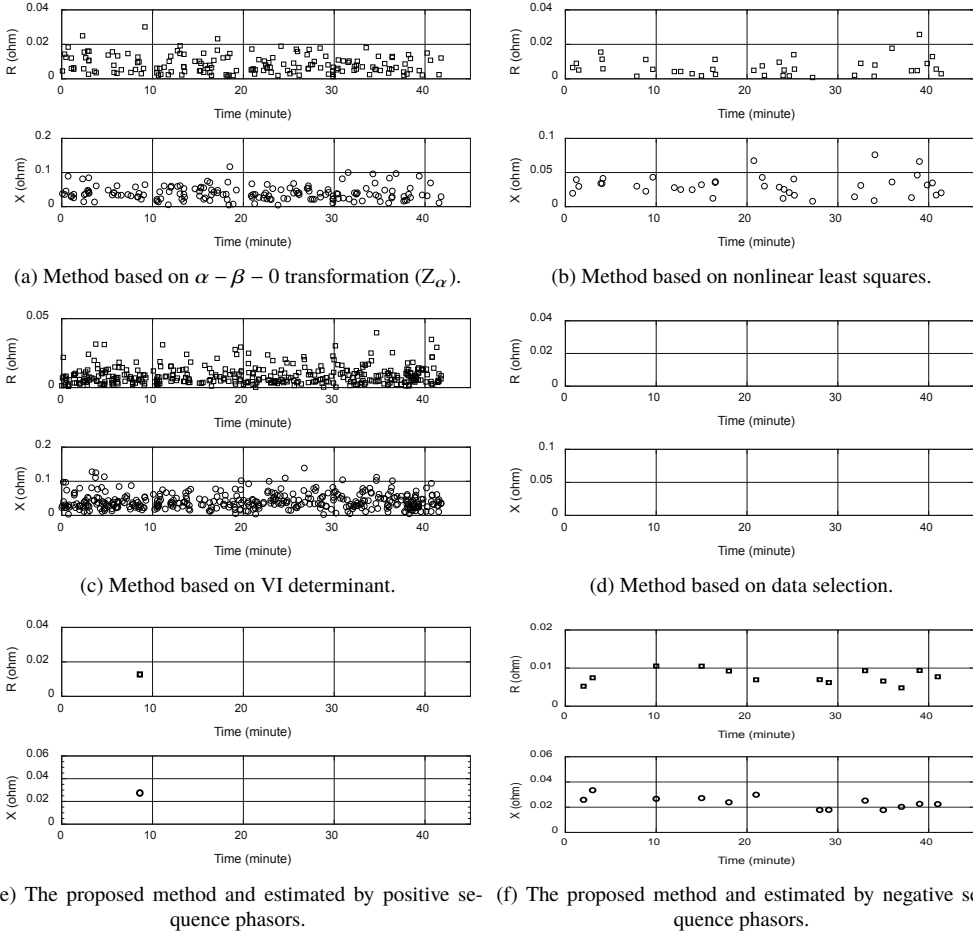


Fig. 13. System impedance estimated results of the oil sand site.

data selection does not provide any reliable results, because all estimates cannot satisfy the data selection requirement.

The system impedances were then estimated by the proposed method with a group of 10 samples and screened according to the criteria developed earlier. The output for every minute was plotted in Figs. 13e–13f, which shows a stream of estimated impedance data. Compared with Fig. 13d, it can be found that the positive sequence quantities are able to yield one feasible result owing to the data regrouping technique. On the other hand, estimation based on negative sequence quantities again leads to more estimates than that of the positive sequence.

The average values of the calculated impedance parameters are presented in Table 7. Since the PSS/E program does not have a detailed secondary distribution system model, the estimated system impedances are validated through a comparison with harmonic impedances. It is observed that the load current contains high 5th and 7th harmonic components. By using the method presented in [27], the site's average 5th harmonic impedance and 7th harmonic impedance are estimated to be $0.012 + 0.110j$ and $0.015 + 0.170j$, respectively. The results suggest that the reference value of the system impedance at the fundamental frequency can be calculated as $Z_s = R_{5th} + X_{5th}/5 = 0.012 + 0.022j$ or $Z_s = R_{7th} + X_{7th}/7 = 0.015 + 0.024j$. This is generally in good agreement with the estimated values.

Table 7. System impedance data of the oil sand site.

	Estimated by negative sequence	Estimated by positive sequence	Reference value (5 th)	Reference value (7 th)
System impedance	$0.011 + 0.025j$	$0.008 + 0.024j$	$0.012 + 0.022j$	$0.015 + 0.024j$

6. Conclusions

A passive method for measuring the supply system impedances has been developed in this paper. Verification studies have been conducted using extensive field data. The results show that the algorithm can estimate system impedances for the majority of cases adequately. The main findings are summarized and discussed as follows:

- The impedance estimation accuracy is improved by regrouping the measurement data, which is intended to find samples with equal system equivalent voltage. An algorithm for removing undesirable transient data and selecting good estimates is also introduced, leading to a reliable impedance estimation method.
- In view of the fact that the network positive sequence impedance is generally equal to its negative sequence impedance, this research has investigated the use of negative sequence components as an additional source of data to improve the positive sequence impedance estimation. The results are satisfactory as more reliable estimates are obtained in most field cases. The recommendation is to rely on the negative sequence components when the load has sufficient negative sequence currents
- The proposed method is verified by a large amount of data. Many field data used in this paper are short-term measurements, such as 45 minutes. Even for such a relatively short period, a number of impedance results have been obtained. This suggests that if one can monitor a site for 24 hours or a few days, many of impedance estimates can be obtained and more reliable results can be determined. In view of the fact that the system impedance does not change a lot over time, we can conclude that for practical purposes the proposed algorithm will be able to meet industrial needs.

- Since load variations can happen at different times, the best strategy for impedance estimation is to perform long term monitoring. The recommendation monitoring period is several days to 1 week. This is especially applicable for cases where load fluctuations are not frequent.

References

- [1] Abdelkader, S. M., & Morrow, D. J. (2014). Online Thevenin equivalent determination considering system side changes and measurement errors. *IEEE Transactions on Power Systems*, 30(5), 2716–2725. <https://doi.org/10.1109/TPWRS.2014.2365114>
- [2] Li, W., Wang, Y., & Chen, T. (2010). Investigation on the Thevenin equivalent parameters for online estimation of maximum power transfer limits. *IET generation, transmission & distribution*, 4(10), 1180–1187. <https://doi.org/10.1049/iet-gtd.2010.0342>
- [3] Dilek, M., Broadwater, R., & Sequin, R. (2003). Calculating short-circuit currents in distribution systems via numerically computed Thevenin equivalents. *Proceedings IEEE PES Transmission and Distribution Conference and Exposition, USA*. <https://doi.org/10.1109/TDC.2003.1335075>
- [4] Cobreces, S., Bueno, E. J., Pizarro, D., Rodriguez, F. J., & Huerta, F. (2009). Grid impedance monitoring system for distributed power generation electronic interfaces. *IEEE Transactions on Instrumentation and Measurement*, 58(9), 3112–3121. <https://doi.org/10.1109/TIM.2009.2016883>
- [5] Patsalides, M., Efthymiou, V., Stavrou, A., & Georghiou, G. E. (2015). Simplified distribution grid model for power quality studies in the presence of photovoltaic generators. *IET Renewable Power Generation*, 9(6), 618–628. <https://doi.org/10.1049/iet-rpg.2014.0231>
- [6] Al-Mohammed, A. H., & Abido, M. A. (2014). An adaptive fault location algorithm for power system networks based on synchrophasor measurements. *Electric Power Systems Research*, 108, 153–163. <https://doi.org/10.1016/j.epsr.2013.10.013>
- [7] Su, H. Y., & Liu, T. Y. (2018). Robust Thevenin equivalent parameter estimation for voltage stability assessment. *IEEE Transactions on Power Systems*, 33(4), 4637–4639. <https://doi.org/10.1109/TPWRS.2018.2821926>
- [8] An, T., Zhou, S., Yu, J., & Zhang, Y. (2006). Tracking Thevenin equivalent parameters on weak voltage load bus groups. *IEEE PES Power Systems Conference and Exposition, USA*. <https://doi.org/10.1109/PSCE.2006.296147>
- [9] Tsukamoto, M., Ogawa, S., Natsuda, Y., Minowa, Y., & Nishimura, S. (2000). Advanced technology to identify harmonics characteristics and results of measuring. *Proceedings of the Ninth International Conference on Harmonics and Quality of Power, USA*. <https://doi.org/10.1109/ICHQP.2000.897051>
- [10] Sumner, M., Palethorpe, B., & Thomas, D. W. (2004). Impedance measurement for improved power quality-part 1: the measurement technique. *IEEE Transactions on Power Delivery*, 19(3), 1442–1448. <https://doi.org/10.1109/TPWRD.2004.829873>
- [11] Wang, W., Nino, E. E., & Xu, W. (2007). Harmonic impedance measurement using a thyristor-controlled short circuit. *IET Generation, Transmission & Distribution*, 1(5), 707–713. <https://doi.org/10.1049/iet-gtd:20060488>
- [12] Czarnecki, L. S., & Staroszczyk, Z. (1996). On-line measurement of equivalent parameters for harmonic frequencies of a power distribution system and load. *IEEE transactions on instrumentation and measurement*, 45(2), 467–472. <https://doi.org/10.1109/19.492769>
- [13] Nagpal, M., Xu, W., & Sawada, J. (1998). Harmonic impedance measurement using three-phase transients. *IEEE Transactions on Power Delivery*, 13(1), 272–277. <https://doi.org/10.1109/61.660889>

- [14] Staroszczyk, Z. (2005). A method for real-time, wide-band identification of the source impedance in power systems. *IEEE Transactions on Instrumentation and Measurement*, 54(1), 377–385. <https://doi.org/10.1109/TIM.2004.838111>
- [15] Langella, R., & Testa, A. (2006). A new method for statistical assessment of the system harmonic impedance and of the background voltage distortion. *International Conference on Probabilistic Methods Applied to Power Systems*, Sweden. <https://doi.org/10.1109/PMAPS.2006.360349>
- [16] Borkowski, D., & Barczentewicz, S. (2014). Power grid impedance tracking with uncertainty estimation using two stage weighted least squares. *Metrology and Measurement Systems*, 21(1), 99–110. <https://doi.org/10.2478/mms-2014-0010>
- [17] Duda, K., Borkowski, D., & Bień, A. (2009). Computation of the network harmonic impedance with Chirp-Z transform. *Metrology and Measurement Systems*, 16(2), 299–312.
- [18] Yang, J., Li, W., Chen, T., Xu, W., & Wu, M. (2010). Online estimation and application of power grid impedance matrices based on synchronised phasor measurements. *IET generation, transmission & distribution*, 4(9), 1052–1059. <https://doi.org/10.1049/iet-gtd.2010.0021>
- [19] Liu, Z., Xu, Y., Jiang, H., & Tao, S. (2020). Study on Harmonic Impedance Estimation and Harmonic Contribution Evaluation Index. *IEEE Access*, 8, 59114–59125. <https://doi.org/10.1109/ACCESS.2020.2982950>
- [20] Wang, B., Ma, G., Xiong, J., Zhang, H., Zhang, L., & Li, Z. (2018). Several sufficient conditions for harmonic source identification in power systems. *IEEE Transactions on Power Delivery*, 33(6), 3105–3113. <https://doi.org/10.1109/TPWRD.2018.2870051>
- [21] Karimi-Ghartemani, M., & Iravani, M. R. (2005). Measurement of harmonics/inter-harmonics of time-varying frequencies. *IEEE Transactions on Power Delivery*, 20(1), 23–31. <https://doi.org/10.1109/TPWRD.2004.837674>
- [22] Xu, W., Ahmed, E. E., Zhang, X., & Liu, X. (2002). Measurement of network harmonic impedances: practical implementation issues and their solutions. *IEEE Transactions on Power Delivery*, 17(1), 210–216. <https://doi.org/10.1109/61.974209>
- [23] Arefifar, S. A., & Xu, W. (2009). Online tracking of power system impedance parameters and field experiences. *IEEE Transactions on Power Delivery*, 24(4), 1781–1788. <https://doi.org/10.1109/TPWRD.2009.2021046>
- [24] Abdelkader, S. M., & Morrow, D. J. (2012). Online tracking of Thévenin equivalent parameters using PMU measurements. *IEEE Transactions on Power Systems*, 27(2), 975–983. <https://doi.org/10.1109/tpwrs.2011.2178868>
- [25] Hui, J., Freitas, W., Vieira, J. C., Yang, H., & Liu, Y. (2012). Utility harmonic impedance measurement based on data selection. *IEEE Transactions on Power Delivery*, 27(4), 2193–2202. <https://doi.org/10.1109/TPWRD.2012.2207969>
- [26] Hui, J., Yang, H., Lin, S., & Ye, M. (2010). Assessing utility harmonic impedance based on the covariance characteristic of random vectors. *IEEE Transactions on Power Delivery*, 25(3), 1778–1786. <https://doi.org/10.1109/TPWRD.2010.2046340>
- [27] Karimzadeh, F., Esmaili, S., & Hosseinian, S. H. (2016). Method for determining utility and consumer harmonic contributions based on complex independent component analysis. *IET Generation, Transmission & Distribution*, 10(2), 526–534. <https://doi.org/10.1049/iet-gtd.2015.0997>
- [28] Zhao, X., & Yang, H. (2015). A new method to calculate the utility harmonic impedance based on FastICA. *IEEE Transactions on Power Delivery*, 31(1), 381–388. <https://doi.org/10.1109/TPWRD.2015.2491644>
- [29] Chen, F., Mao, N., Wang, Y., Wang, Y., & Xiao, X. (2019). Improved utility harmonic impedance measurement based on robust independent component analysis and bootstrap check. *IET Generation, Transmission & Distribution*, 14(5), 910–919. <https://doi.org/10.1049/iet-gtd.2019.1153>

- [30] IEEE Standards Association (2009). *IEEE Recommended Practice for Monitoring Electric Power Quality* (IEEE Standard 1159-2019), 1–98. <https://doi.org/10.1109/IEEESTD.2019.8796486>
- [31] Borkowski, D., & Bien, A. (2009). Improvement of accuracy of power system spectral analysis by coherent resampling. *IEEE Transactions on Power Delivery*, 24(3), 1004–1013. <https://doi.org/10.1109/TPWRD.2009.2013662>



Shuangting Xu received the B.S. degree in electrical engineering and its automation from the College of Electrical Engineering, Sichuan University, Chengdu, China, in 2016, where she is currently working toward the Ph.D. degree in power systems and their automation. Her main research interest is power system harmonic analysis.



Yang Wang received the B.S. degree in electrical engineering from Zhejiang University, Hangzhou, China, in 2012 and the Ph.D. degree in electrical and computer engineering from the University of Alberta, Edmonton, Canada, in 2017. He is currently a Research Fellow with the College of Electrical Engineering, Sichuan University, Chengdu, China. His main research interests are power quality and integration of renewables.



Xianyong Xiao received the Ph.D. degree from Sichuan University, Chengdu, China, in 2010. He is a Professor and Dean with the College of Electrical Engineering, Sichuan University, China. His research interests include power quality and its control, distribution system reliability, and eco-friendliness.



Jun Wu received the B.S. and M.S. degrees in electrical engineering from the College of Electrical Engineering, Zhejiang University, Hangzhou, China, in 2001 and 2004, respectively. He is currently a Senior Engineer with the Electric Power Research Institute of the State Grid Zhejiang Electric Power Company, LTD. His main research interest is power quality.